

# Effect of Crystallization and Interface Formation Mechanism on Mechanical Properties of Film-Insert Injection-Molded Poly(propylene) (PP) Film/PP Substrate

S. Yamaguchi,<sup>1</sup> Y. W. Leong,<sup>2</sup> T. Tsujii,<sup>3</sup> M. Mizoguchi,<sup>4</sup> U. S. Ishiaku,<sup>2</sup> H. Hamada<sup>2</sup>

<sup>1</sup>Materials R&D Department, Daihatsu Motor Co. Ltd., 3000, Yamanoue, Ryuo, Gamo, Shiga 520-2593, Japan

<sup>2</sup>Advanced Fibro-Science, Kyoto Institute of Technology, Matsugasaki Sakyo-ku, Kyoto 606-8585, Japan

<sup>3</sup>PerkinElmer Japan Co. Ltd., 5-3, Toyotsu-cho, Suita, Osaka 564-0051, Japan

<sup>4</sup>Department of Polymer Science and Engineering, Yamagata University, Jonan, Yonezawa, Yamagata 992-8510, Japan

Received 10 March 2004; accepted 12 October 2004

DOI 10.1002/app.21590

Published online in Wiley InterScience (www.interscience.wiley.com).

**ABSTRACT:** A previous study has shown that the adhesion between the film and substrate of film-insert injection-molded poly(propylene) (PP) film/PP substrate was evident with the increases in barrel temperature and injection holding pressure. In this second part of the research work, the crystallinity at the interfacial region (i.e., region between the film and the injected substrate) was extensively studied using FTIR imaging, polarized light microscopy, and DSC in an attempt to determine the level of influence that crystallinity has on the interface and bulk mechanical properties. Consequently, a more thorough and clearer picture of the influence of the inserted film on the interfacial crystallinity and subsequently the substrate mechanical properties, such as peel strength and impact strength, has been revealed. The initial proposition that crystallinity could enhance film–substrate interfacial bonding has been confirmed, judging from the higher peel strength with increasing crystallinity at the

interfacial region. Nevertheless, the change in crystallinity was not only confined to the interfacial region. With the film acting as heat-transfer inhibitor between the injected resin and the mold wall, the total crystal structure of the substrate was substantially altered, which subsequently affected the bulk mechanical properties. The lower impact strength of film-insert injection-molded samples compared to that of samples without film inserts provided evidence of how the film could impart inferior properties to the substrate. The difference in cooling rate between the substrate and film might also cause other defects such as warpage and/or residual stress build-up within the product. © 2005 Wiley Periodicals, Inc. *J Appl Polym Sci* 98: 294–301, 2005

**Key words:** films; molding; poly(propylene) (PP); crystallization; morphology

## INTRODUCTION

The crystallinity of postprocessed polymeric materials has undoubtedly received much attention because of its strong influence on both mechanical and optical properties of the end product. Crystal formation in semicrystalline polymers has been reported to be affected by various factors including incorporation of nucleating agents and fillers,<sup>1–4</sup> transcrystallinity at fiber–matrix interfaces,<sup>5–7</sup> high shear with other surfaces such as mold walls,<sup>8</sup> and processing conditions.<sup>9</sup>

With the advent of new injection-molding technology, current molded products, besides gaining increasing complexity in shape, are also becoming more fanciful and striking in terms of appearance. Manufacturers nowadays are using relatively new and cost-effective techniques to mold high-quality products that also incorporate durable and colorful surface designs. This technique is called film-insert injection

molding or sometimes only referred to as film-insert molding (FIM). The FIM technique has thus far gained popularity because it eliminates postmolding processes such as spray painting or heat-induced labeling, which would obviously cost more.<sup>10–14</sup> Furthermore, the FIM technique, which has already been patented,<sup>15–18</sup> is relatively simple, whereby a pre-printed and preformed film is inserted into the mold before a resin is injected into the mold to form the substrate. The hot resin would usually wet and partially melt the film, which would cause adhesion of the film to the substrate after the product is cooled. The extent of adhesion, as previously studied, depends on various factors such as barrel temperature, injection speed, injection holding pressure, and the miscibility between the materials of the substrate and the film. In our estimation, however, studies and observations on the effects of crystallinity at the film–substrate interfacial region on film–substrate adhesion and bulk mechanical properties are still in just a rudimentary stage. Thus, a more comprehensive investigation has been carried out to characterize the thermal properties at and around the film–substrate interfacial region and subsequently correlate it to the changes in adhesion

Correspondence to: Y. Leong (leongyewwei@hotmail.com).

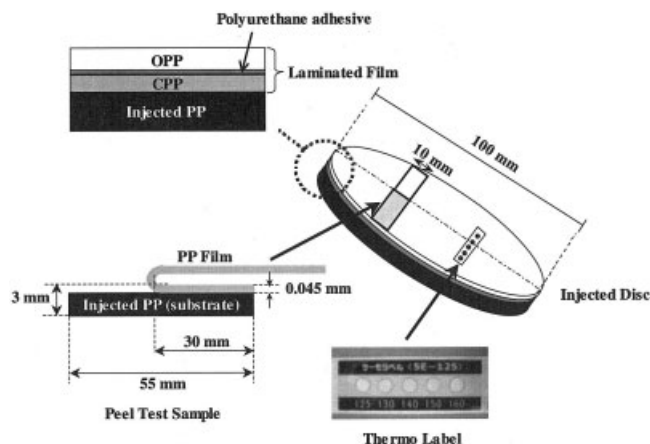


**Figure 1** Schematic of the injection-molded disc, showing preparation and geometry of peel test samples, composition of the laminated film, and the position of thermolabel attachment.

and bulk mechanical properties caused by the film insert.

## EXPERIMENTAL

### Materials

The injection resin used in this study was a PP block copolymer, consisting of propylene and ethylene (J104WA; Mitsui Chemical Co. Ltd., Tokyo, Japan), whereas PP film (Toyobo Co. Ltd., Osaka, Japan) was used as the insert. The film was supplied as a laminate; that is, oriented-PP (OPP) and cast-PP (CPP) adhered by polyurethane, as shown in Figure 1. Both films possess an average molecular weight of about 300,000. Thicknesses of OPP and CPP were 20 and 25  $\mu\text{m}$ , respectively.

### Thermal analysis

Thermal properties of the laminated film and injection resin were measured by differential scanning calorimetry (DSC7; Perkin Elmer Cetus Instruments, Nor-

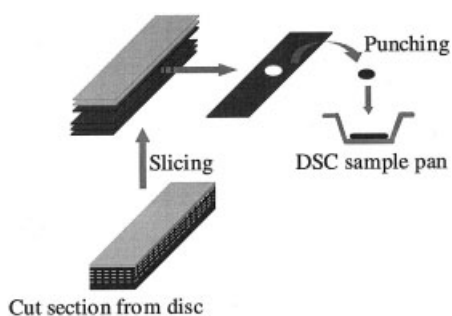


**Figure 2** Schematic showing the slicing of a portion of the injection-molded disc, and subsequently punching the sliced sample for DSC analysis.

**TABLE I**  
Molding Conditions

Barrel temperature	200, 210, 220°C
Injection speed	40 mm/sec
Holding pressure	25 MPa
Holding time	15 s
Mold temperature	40°C

walk, CT). The sample was heated from 30 to 200°C (first heating), cooled to 30°C, and heated again to 200°C (second heating), all at the rate of 10°C/min. DSC samples were also taken from the molded disc by slicing a section of the disc using a microtome (Reichert Ultracut-S; Leica, Wetzlar, Germany) at -30°C and later punching the slice to fit the DSC sample pan, as shown in Figure 2. The thickness of the sliced sample was about 20  $\mu\text{m}$  and DSC analysis was carried out under nitrogen atmosphere. Temperature scan was from 30 to 200°C, at a rate of 10°C/min.

### Injection molding

PP resin was injected into a disc-shape cavity mold to produce disc samples, as shown in Figure 1, using a J110CEL III (The Japan Steel Works, Ltd., Tokyo, Japan) injection-molding machine. The film was attached to one side of the mold wall before injection. The molding conditions are indicated in Table I. The barrel temperature was varied to investigate the effect of temperature on crystallization and interface formation. Moldings with no film inserts were also prepared as a control.

Because there is a possibility that the temperature at which the injected resin touches the film (interfacial temperature) is dissimilar to the set barrel temperature, thermolabels (Nichiyu Giken Kogyo Co. Ltd., Tokyo, Japan) were attached to the film before injection molding, as shown in Figure 1, to determine the exact interfacial temperature. The interfacial temperatures recorded by the thermolabels versus the various barrel temperatures are listed in Table II. The determination of the interfacial temperature is vital because crystal formation at the interfacial region is highly dependent on this temperature.

### Morphological analysis

The crystal structure of the injected resin at the film-substrate interfacial region was observed using a po-

**TABLE II**  
Measured Interfacial Temperatures According to Set Barrel Temperatures

Barrel temperature (°C)	Interfacial temperature (°C)
200	120
210	130
220	140

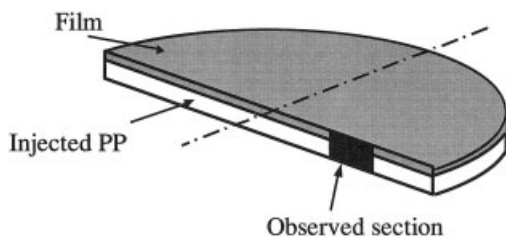


**Figure 3** Schematic depicting the section observed using a polarized light microscope.

larized light microscope (BHS-751P; Olympus, Osaka, Japan). The samples were cross-sectioned parallel to the melt flow direction, as shown in Figure 3. The cross section was then sliced to a thickness of  $20\ \mu\text{m}$  by using a microtome (Reichert Ultracut-S) at  $-30^\circ\text{C}$ .

Crystallinity distribution around the interfacial region was measured using an imaging FTIR system (Spectrum Spotlight 300; Perkin-Elmer). The samples were also prepared by slicing to  $10\ \mu\text{m}$  thickness. The resolution was set at  $4\ \text{cm}^{-1}$ , the scanning range was at wavenumbers from  $4000$  to  $720\ \text{cm}^{-1}$ , and the number of scans was four. Crystallinity was calculated as the ratio of absorbance of the crystal band ( $998\ \text{cm}^{-1}$ ) to the amorphous band ( $974\ \text{cm}^{-1}$ ).

#### Morphological observation of the interface

Internal structure around the interface was observed by transmission electron microscopy (TEM). The samples were prepared by slicing using a microtome similar to that used in preparing samples for polarization microscopy, as shown in Figure 2, although the thickness of the samples here was only  $100\ \text{nm}$ . Before observation, the samples were immersed into  $\text{RuO}_4$  solution for 10 h at room temperature to dye the sample. TEM used was H-8100 (Hitachi, Osaka, Japan) at 100-kV accelerated voltage and  $\times 150,000$  magnification.

#### Deductions concerning film molecular orientation

Changes in molecular orientation in the film were deduced by means of observations based on thermal and tensile properties of heat-treated film. Films were subjected to heat treatment, ranging from  $100$  to  $150^\circ\text{C}$ , by using a heat-sealing machine (Fuji Impulse Co. Ltd., Osaka, Japan), as shown in Figure 4, to simulate the conditions to which the film was subjected during injection molding. The heat-treatment temperatures were chosen based on the interfacial temperatures recorded by the thermolabels. The heat-treated films were then tensile tested to gauge the effect of heat-treatment temperature on the film's mechanical properties.

DSC analyses were also carried out on the heat-treated films using the same conditions set for non-

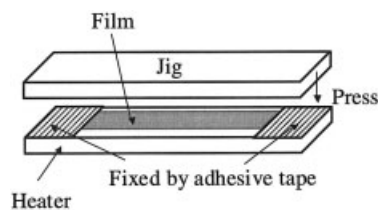


**Figure 4** Schematic of the heat-treatment process on a film using a heat-sealing machine.

heat-treated films, to determine their heat of fusion, calculated as the area under the melting curve. The normalized heat of fusion of all the samples would then be compared to observe any changes in crystallinity arising from different heat-treatment temperatures.

## RESULTS AND DISCUSSION

#### Preliminary thermal analysis

A preliminary thermal analysis was done on the as-received film and resin to determine the basic thermal properties of the raw materials. Plots of the DSC exothermic and endothermic curves are shown in Figure 5. The first heating endothermic curve of the laminated film shows two melting peaks,  $149$  and  $167^\circ\text{C}$ , corresponding to the melting points of CPP and OPP, respectively. In the second heating curve, however, the melting peaks of CPP and OPP shifted to  $147$  and  $160^\circ\text{C}$ , respectively. The reason behind the shift in

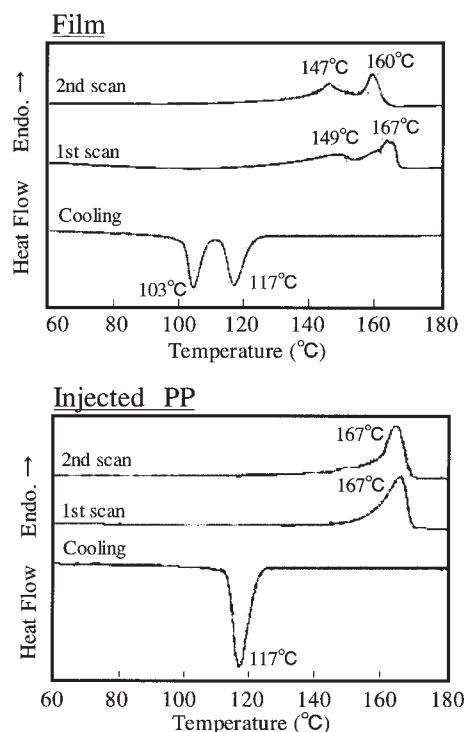


**Figure 5** DSC results of the as-received film and PP resin.

melting points is that the second heating curve corresponds to the true characteristics of the films, given that all the processing history has been erased after the first heating. In the cooling curve, two exothermic peaks around 103 and 117°C were observed, corresponding to the crystallization temperatures of CPP and OPP, respectively.

Meanwhile, the first and second heating scans of PP resin did not yield significant changes, suggesting that past processing conditions did not have much influence on the crystal structure of the resin. Thus, it can be assumed that the films are more prone to crystallinity and/or molecular orientation changes when subjected to different processing conditions.

### Film–substrate interfacial crystallinity

The polarized light micrographs in Figure 6 show the comparison of the crystal sizes in the substrates between specimens molded with and without the film insert. The morphology of the specimen molded without the film insert clearly shows very minimal crystal growth, especially at the regions adjacent to the mold wall. The sight of small but numerous crystals at this region indicates that the rapid heat transfer from the resin melt to the cold mold wall has deprived the nuclei in the substrate of the energy needed to form crystals, and thus the formation and growth of crystals have been suppressed. A typical phenomenon in injection-molded products would indicate larger crystal sizes with increased distance from the mold wall, as the cooling rates of the polymer melt gradually decrease with distance.

On the other hand, large crystal formations are apparent throughout the substrate in specimens containing the film insert, suggesting that there is enough energy (heat) for the nuclei to form into coarser crystals. This would attest to the fact that the film has acted as an insulator, obstructing heat flow from the melt to the mold. Thus, a higher crystallinity at this region can be expected.

The crystallinity distribution around the film–substrate interfacial region recorded using the imaging FTIR technique is shown in Figure 7. The darker and lighter regions correspond to low and high crystallinity areas, respectively. It is obvious that the images agree well with the results obtained from polarized light microscopy. A generally low crystalline region can be seen in samples molded without the film insert, whereas a higher crystallinity level was observed in the substrate of film-insert-molded samples. Moreover, it is also clear from the images that the crystallinity of the films changed as well corresponding to the increase in barrel temperature. At lower barrel temperatures, only the outermost region of the film that touches the injected resin would be affected because the interfacial temperature is barely sufficient even to melt, let alone cause alteration to, the crystal

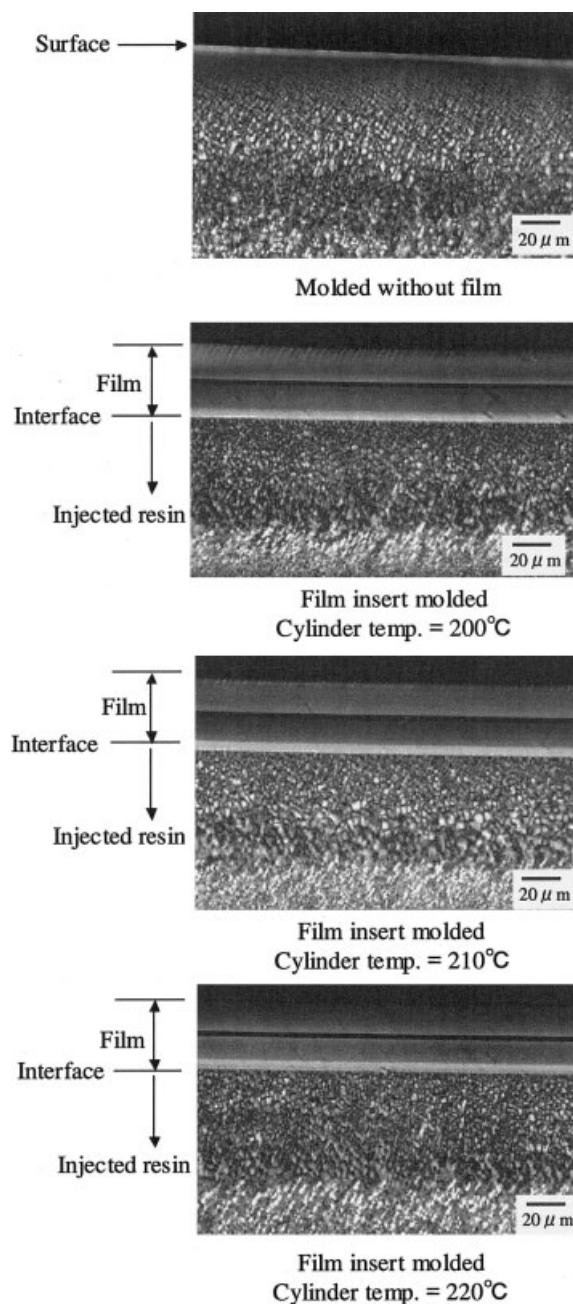


**Figure 6** Polarized light micrographs comparing the crystal structure at the surface of normal injection-molded to the film–substrate interfacial regions of film-insert injection-molded samples.

structure of the film. However, at higher barrel temperatures, the heat from the injected resin would at least partially melt the film, thus causing both rearrangement of molecular chains and interdiffusion between the film and substrate. Nevertheless, it is important to note that the FTIR images represent only qualitative assessments of the crystallinity around the said regions.

To quantitatively characterize the crystallinity around the interfacial regions, the samples were sliced by microtome and DSC analysis was performed on

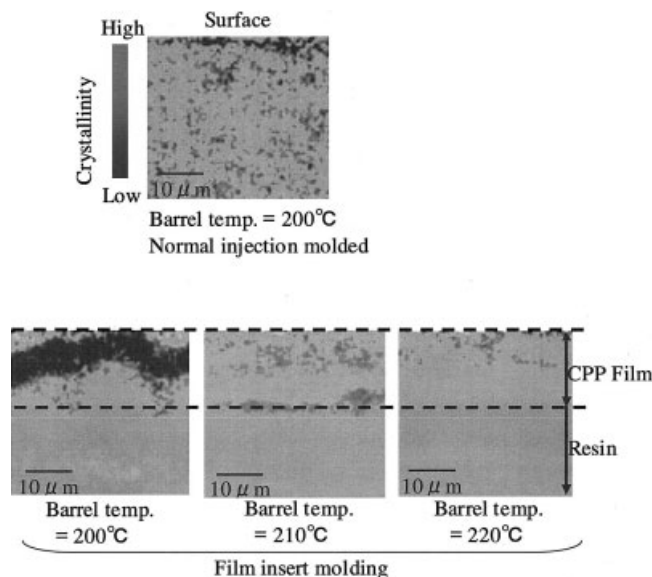


**Figure 7** Imaging FTIR images depicting the crystallinity distribution of a normal injection-molded and film-insert injection-molded samples.

each slice to determine the heat of fusion, which is representative of the amount of crystallinity. DSC results, as depicted in Figure 8, show the relationship between the heat of fusion and the distance from the surface of the specimen. The surface of the specimen, in this case, points to either the surface adjacent to the mold wall for specimens molded without film insert, or the surface adjacent to the film for film-insert-molded specimens. In specimens that were molded without film inserts, the surface crystallinity was substantially low, judging from the low heat of fusion recorded. Crystallinity would then gradually increase with distance toward the core of the specimen. This is in agreement with the results obtained earlier from polarized light microscopy observations.

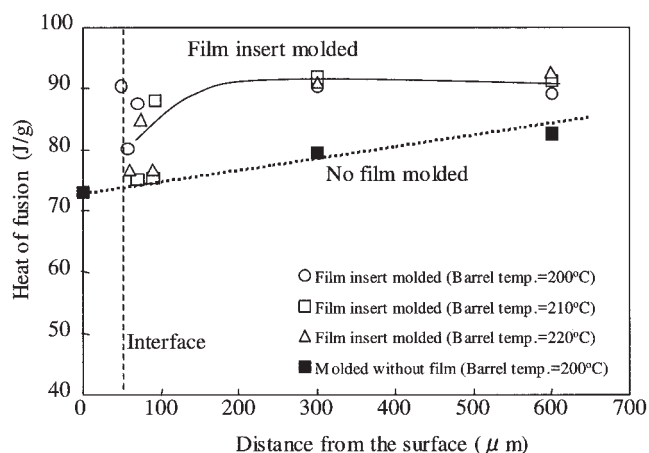


**Figure 8** Comparison of the heat of fusion of substrates through thickness direction between normal injection-molded and film-insert injection-molded samples.

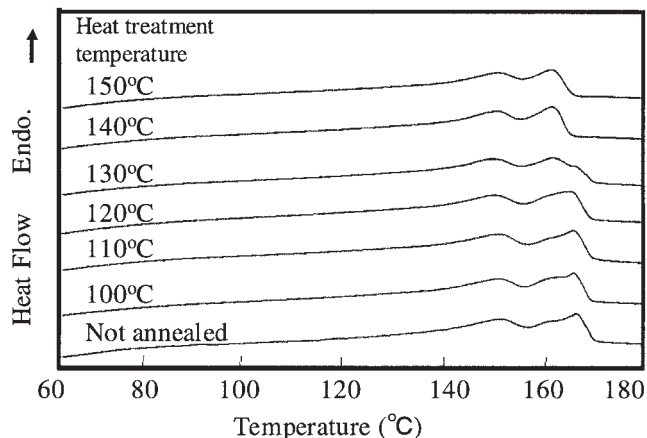


**Figure 9** DSC heating curves films before and after heat treatment at various temperatures.

In film-insert-molded specimens, the heat of fusion in all positions was higher than that of specimens molded without films. Although an increase in crystallinity could still be noted, the gradient of increase is not as sharp as that recorded in no-film specimens. It is also noteworthy that around the film-substrate interfacial region, the recorded heats of fusion data are quite scattered. This might be attributable to the influence of CPP in the film, which has very low crystallinity compared to that of either OPP or the injected resin, thus significantly lowering some of the readings. This problem would mainly surface in high barrel temperature specimens as the films begin to melt.

The results shown here confirm the observation from a previous work,<sup>19</sup> that the higher crystallinity of the substrate in film-insert specimens has contributed to enhanced brittleness and lower impact properties.

### Deduction of film molecular orientation

With the aim of substantiating the claims from a previous study that the properties of the film have an overall effect on the film-substrate adhesion and bulk mechanical properties, a thorough study was done to determine the state of molecular orientation of the film before and after injection molding. The films were subjected to heat treatment in a heat-sealing machine to simulate the actual conditions during injection molding. Figure 9 compares the DSC curves of heat-treated film with those of the original (as-received) film. Below the heat-treatment temperature of 130°C, two endothermic peaks around 149 and 167°C were derived, corresponding to the melting peaks of CPP and OPP, respectively. Beyond a heat-treatment temperature of 130°C, the OPP melting peak shifted to 160°C, whereas no change was recorded in the melting peak of CPP. Thus, it is believed that during injection molding, molecular orientation in OPP would be altered at an interfacial temperature of >130°C. Thus,

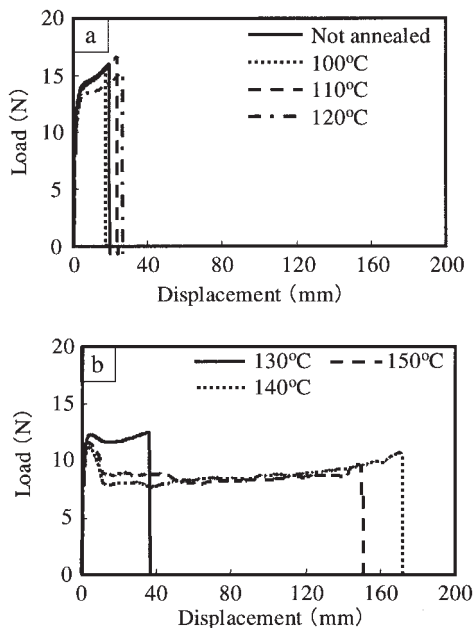


**Figure 10** Load–displacement curves of films before and after heat treatment.

the films (untreated and heat-treated) were subjected to tensile tests to determine whether the altered molecular orientation in OPP affected their tensile properties.

Figure 10 shows the tensile load–displacement curves of untreated and heat-treated films. The graphs were separated to segregate the specimens that have almost similar patterns from those that have different patterns. Figure 10(a) shows the load–displacement curves of specimens that were untreated and heat-treated below 130°C (i.e., 100, 110, and 120°C). Here, the curve patterns for all specimens are obviously quite similar, whereby initially the load increased sharply up to about 13 N; thereafter the films yielded while the load continued to increase gradually until the film breaks with a displacement range of 20 to 30 mm.

Figure 10(b) shows specimens that are heat-treated at and above 130°C. It is apparent that the curves shown in this figure are very different from those depicted in Figure 10(a). For the specimen heat-treated at 130°C, although the load at yield has not changed significantly (13 N), the film seemed to have elongated further before breaking at a displacement of about 40 mm. Furthermore, specimens heat-treated at 140 and 150°C recorded displacements of up to 170 mm, which is distinctly different from those previously recorded by other samples. At this point, it is strongly believed that the increase in interfacial temperature has caused the film, especially the OPP region, to partially melt, thus losing its orientation (molecular chain relaxation) upon cooling. It is also clearly visible that the yield strengths of the films are still intact, all of which

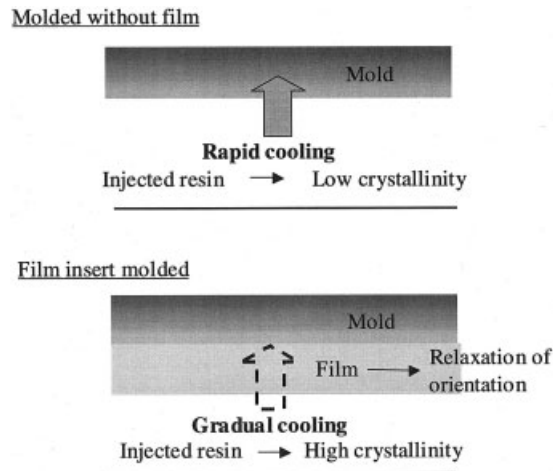


**Figure 11** Model representing the heat-transfer mechanism during injection molding that affects the crystal structure of substrates in normal and film-insert injection-molded samples.

would yield at approximately 13 N. Although the reason behind this phenomenon is still unclear, this indicates that the films still retain their elasticity even though the molecular orientation of the films has been altered. A model has thus been proposed in Figure 11 to give an insight into the crystalline nature at the interfacial region. This is a very interesting and important observation because film–substrate debonding (peeling) would almost always start at or below the film’s yield point according to observations in a previous study. Another interesting point to note is that, because the molecular structure of OPP changes at the interfacial temperature of 130°C, good bonding between the film and substrate can be expected. This correlates well with the peel test results conducted during a previous study.<sup>19</sup>

As expected, the altered molecular orientation does not come without compromising the films’ strength. Figure 12 shows the relationship between load at break and heat-treatment temperature. Molecular chain relaxation arising from the increase in

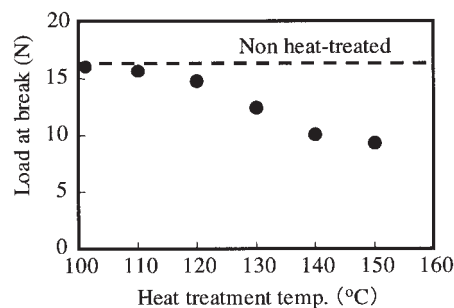


**Figure 12** Load at break of films before and after heat treatment at various temperatures.

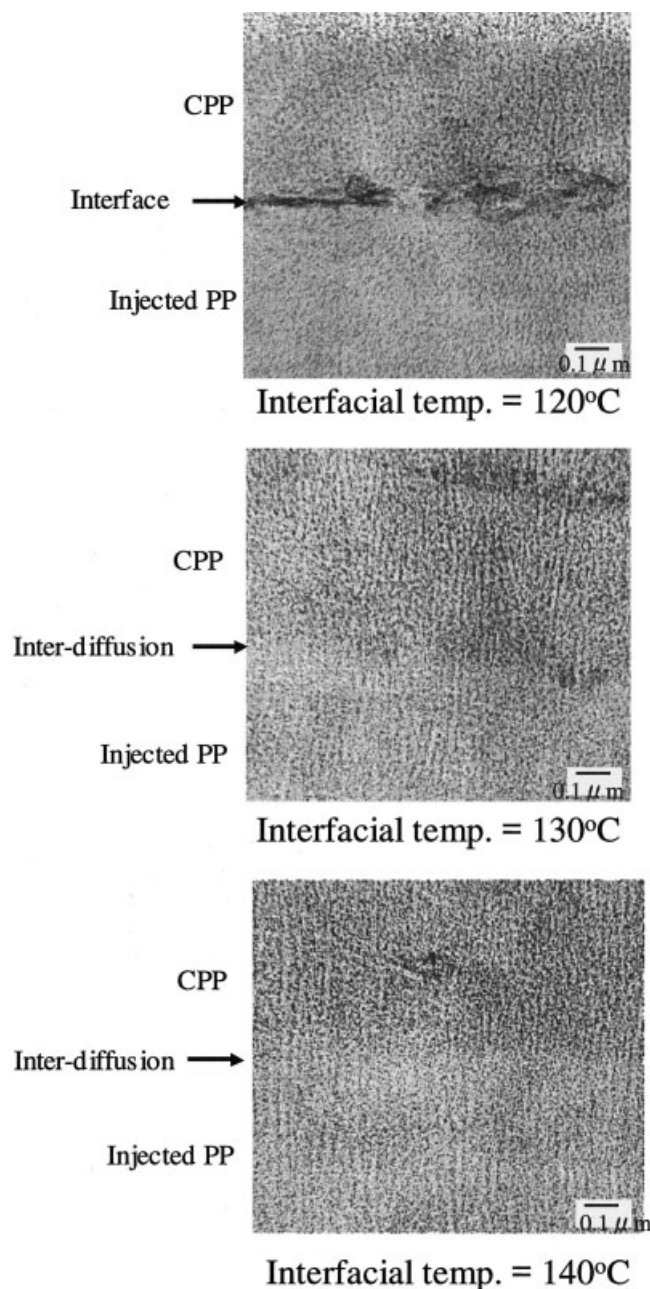


**Figure 13** TEM micrographs showing the formation (or fading) of the film-substrate interface at various interfacial temperatures.

heat-treatment temperature has unduly caused the film to lose its load-bearing properties and subsequently failing at a lower load.

#### Mechanism of interface formation

The formation mechanism of film-substrate interface formation can be further understood by observing the morphologies generated using TEM, as depicted in Figure 13. At low interfacial temperature, a large gap at the interface can be observed, which undoubtedly indicates the weak bonding between the film and sub-

strate. With the increase in interfacial temperature, however, it is apparent that this gap has reduced considerably and finally the line indicating the interfacial boundary would diminish. The elimination of this boundary is believed to be the key to obtaining ultimate bonding strength between the film and substrate.

#### CONCLUSIONS

The results in this study have helped to erase doubt and speculations from a previous study that crystallinity at the film-substrate interface could influence the bulk mechanical properties (impact strength) and film-substrate adhesion (peel strength). It was proven that the film indeed altered the crystalline structure of the injected resin because it acted as an insulator that obstructs heat flow from the resin to the mold, consequently leading to the substrate's being cooled at a much slower but gradual rate. Thus, a more crystalline substrate would naturally yield lower impact properties, which is consistent with the results obtained in previous works. The injected resin has in turn modified the molecular orientations in the film, typically when the barrel temperature was set to a high level. Relaxation of molecular chains caused the film to undergo deterioration in terms of tensile strength, although for some unknown reason, the elasticity of the film was maintained. Another interesting fact is that only the OPP layer of the laminated film seems to be affected by the heat, and thus it is believed that the ability of the film to adhere to the substrate strongly depends on how the molecular orientations of this layer are manipulated.

#### References

1. Leong, Y. W.; Mohd. Ishak, Z. A.; Ariffin, A. *J Appl Polym Sci* 2004, 91, 3315.
2. Leong, Y. W.; Mohd. Z. A.; Ishak, Ariffin, A. *J Appl Polym Sci* 2004, 91, 3327.
3. Alonso, M.; Velasco, J. I.; de Saja, J. A. *Eur Polym Mater* 1997, 33, 255.
4. Saujanya, C.; Radhakrishnan, S. *Polymer* 2001, 42, 6723.
5. Bhattacharyya, A. R.; Sreekumar, T. V.; Liu, T.; Kumar, S.; Ericson, L. M.; Hauge, R. H.; Smalley, R. E. *Polymer* 2003, 44, 2373.
6. Assouline, E.; Wachtel, E.; Grigull, S.; Lustiger, A.; Wagner, H. D.; Marom, G. *Polymer* 2001, 42, 6231.
7. Manchado, M. A. L.; Biagiotti, J.; Torre, L.; Kenny, J. M. *Polym Eng Sci* 2000, 40, 2194.
8. Kumaraswamy, G.; Verma, R. K.; Issaian, A. M.; Wang, P.; Kornfield, J. A.; Yeh, F.; Hsiao, B. S.; Olley, R. H. *Polymer* 2000, 41, 8931.
9. Lee, T. H.; Boey, F. Y.C.; Khor, K. A. *Compos Sci Technol* 1995, 53, 259.
10. Wielpuetz, M.; Michaeli, W. ANTEC 2001, Proceedings of the 59th Annual Technical Conference and Exhibition, Society of Plastics Engineers, Dallas, TX, May 7-10, 2001; p 337.

11. Rotheiser, J. I. ANTEC 2001, Proceedings of the 59th Annual Technical Conference and Exhibition, Society of Plastics Engineers, Dallas, TX, May 7–10, 2001; p 553.
12. Applegate, J. ANTEC 2001, Proceedings of the 59th Annual Technical Conference and Exhibition, Society of Plastics Engineers, Dallas, TX, May 7–10, 2001; p 925.
13. Schuering, K. ANTEC 2002, Proceedings of the 60th Annual Technical Conference and Exhibition, Society of Plastics Engineers, San Francisco, CA, May 5–9, 2002; p 526.
14. Kakarala, N.; Pickett, T. ANTEC 2003, Proceedings of the 61st Annual Technical Conference and Exhibition, Society of Plastics Engineers, Nashville, TN, May 5–6, 2003; p 4710.
15. Yamato, H. U.S. Pat. 5,599,608 (1997).
16. Yamato, H. U.S. Pat. 5,746,962 (1998).
17. Yamato, H. U.S. Pat. 5,783,287 (1998).
18. Lilly; Lee, K. U.S. Pat. 6,682,805 (2004).
19. Leong, Y. W.; Yamaguchi, S.; Mizoguchi, M.; Hamada, H.; Ishiaku, U. S.; Tsujii, T. *Polym Eng Sci* 2004, 44, pp 2327–2334.